CrossMark

Metal contact quenching mechanism of sintered $SrAl_2O_4$:Eu^{2+}, Dy^{3+} composite coating

Ling He[1] · Xueyan Wu[1] · Wensheng Li[1] · Shuncai Wang[1] · Qiankun Li[1]

Abstract The self-sensing tribological composite coating (Cu-14Al-X/$SrAl_2O_4$:Eu^{2+}, Dy^{3+}) for wear indicator is quenched because of vacuum pressure-assisted sintering method, which do harm to the monitoring of coating. In this paper, we constructed a model to explain the quenching mechanism of $SrAl_2O_4$:Eu^{2+}, Dy^{3+} in alloy coatings. The initial electron concentration and the energy level structures were studied. The results show that contact quenching rather than the traditional thermal quenching is the most important influencing factor for $SrAl_2O_4$:Eu^{2+}, Dy^{3+}. The contact metal in coatings can be as a defect level and dissipation center of electron transition, the quenching process could be well explained by the model we proposed.

1 Introduction

Persistent luminescent material $SrAl_2O_4$:Eu^{2+}, Dy^{3+} exhibit excellent properties, such as high quantum efficiency, long persistence of phosphorescent, safety and good stability [1, 2] and fields for practical applications including luminescent paint, screens, glow signs, emergency escape routes, detection of structural damage, etc [3, 4]. The copper–aluminum alloy powders have been applied in resisting wear coating due to their excellent mechanical properties and abrasion resistance behavior. In this paper, the Cu-14Al-X [5, 6] was coupled with $SrAl_2O_4$:Eu^{2+}, Dy^{3+} phosphorescence forming the composite coating, which developed a

simple and economic coating monitoring technology. The light-emitting properties of the novel coating can serve as an indicator layer, which warns when the coating has worn off, replacing or recoating is necessary [7]. When we inspect on coating with a hand-held UV-lamp, the yellow-green light of $SrAl_2O_4$:Eu^{2+}, Dy^{3+} will disappear. It means that the functional coating is worn out and that recoating is needed [8].

The Cu-14Al-X/$SrAl_2O_4$:Eu^{2+}, Dy^{3+} composite coating has been successfully prepared by vacuum pressure-assisted sintering method. But the phosphorescent particles are quenched bucause of the preparation method, which will be harmful to the indication of the coating. The quenching behavior of phosphors has been previously studied. For example, Chithambo [9] reported thermal quenching of $SrAl_2O_4$:Eu^{2+},Dy^{3+} with an activation energy and Mothudi [10] proposed hole trap levels when the $SrAl_2O_4$:Eu^{2+}, Dy^{3+} phosphors annealed at different temperatures. Ju Guifang [11] proposed the concentration quenching of Eu^{2+} is attributed to competitive capturing of electrons with traps. Yang XF [12] studied quenching on iron impurity in Eu^{2+}, Dy^{3+} doped strontium aluminates phosphor and explained that iron displace the aluminum and form Fe–O bond. However, most of researches focus on the fluorescent quenching mechanism in the synthesis process. To the best of our knowledge, the report on quenching mechanism of $SrAl_2O_4$:Eu^{2+}, Dy^{3+} coupled with the wear-resistant materials is rare. In this work, luminescent composite coatings doped with rare earth phosphorescence were fabricated by vacuum pressure-assisted sintering. There are five types of composite coatings, which formed by luminescent powders dispersed throughout different matrixes (Cu, Fe, Ni, Mn and Cu-14Al-X). The sintered temperatures and metal contact were investigated in details; also the quenching mechanism of phosphor is discussed in composite coating.

✉ Ling He
hlswm@163.com; 839941113@qq.com

1   State Key Laboratory of Advanced Nonferrous Materials
     Process and Recycles, Lanzhou University of Technology,
     Lanzhou 730050, People's Republic of China

Table 1 Alloy powder composition ratio (mass fraction number)

Alloy content	Al	Cu	Fe	Mn	Co	Ni	Else
Mass fraction	12–14	70–80	2–4	0.8–2.0	0.5–2.5	0.2–0.5	0.5–2.0

Table 2 Experimental program and sintering process

Program	Metal powder	Temperature/°C	Substrates
1	Cu-14A1-X	650/700/800/850	no
2	Cu-14A1-X/Cu/Ni/Fe/Mn	850	45# steel

2 Experimental

2.1 Materials

Ten-millimeter cube 45 # steel substrates were ultrasonically degreased and with alcohol as solvent cleaning. Phosphor $SrAl_2O_4:Eu^{2+}$, Dy^{3+} were purchased commercial spherical fluorescent powder, select 270–360 mesh particle size (particle size 40–53 μm), which has shown irregular grains and free of other impurities. Cu-14A1-X powder was prepared by gas atomization method; the main component of the powder is shown in Table 1. Copper powder, nickel powder, iron powder, manganese powder are commercial electrolytic powder.

2.2 Coating preparation

The powder samples of various metals with 30 vol% phosphor and a certain amount of liquid paraffin as a type agent were mixed for 120 min in three-dimensional vortex mixer. After that, the powder mixtures were put into a graphite die lined with a flexible graphite foil. Powder sintering was proceeded in a RYJ-2000Z type hot pressing (HP) furnace at different temperatures, different pressures. Finally, the hot press chamber was cooled down naturally at an average rate of 10 °C/min. Experimental program and sintering process is shown in Table 2. Before testing, the samples were mechanically polished to 2000 grit Sic paper, and then cleaned ultrasonically with ethyl alcohol.

2.3 Characterization

Phase identification of the coatings was carried out by X-ray diffract meter (D/MAX 2500PC), using Cu a radiation over the 2θ range of 10°–90° with a step width of 6°/min. The accelerating voltage and emission current were 35 kV and 200 mA, respectively. The optical spectra were measured by the fluorescence spectrometer (F-97) with Xe lamp as excitation source at the room temperature.
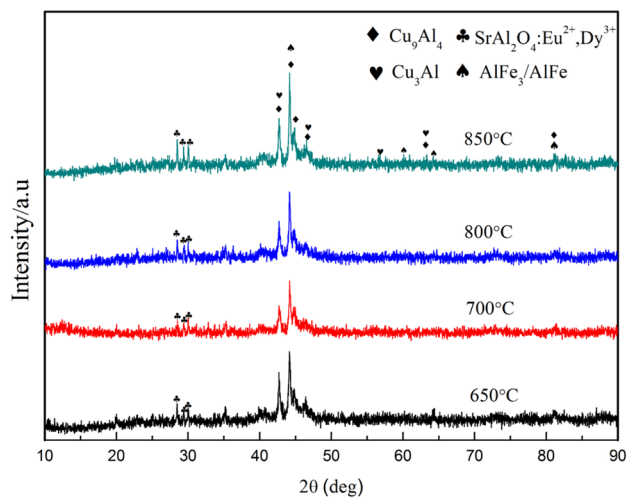
Fig. 1 XRD patterns for Cu-14Al-X/$SrAl_2O_4$:Eu^{2+}, Dy^{3+} coatings at different sintering temperatures

3 Results and discussion

3.1 Crystal structure characterization

Figure 1 shows XRD patterns of Cu-14Al-X/$SrAl_2O_4$: Eu^{2+}, Dy^{3+} composite coatings produced at different sintered temperatures. The XRD profiles indicate that the main phases are Cu_9Al_4 and Cu_3Al and a small amount of $AlFe_3$ phase also exists in Cu-14Al-X/$SrAl_2O_4$:Eu^{2+}, Dy^{3+} composite coatings. In addition, with the increase of sintering temperature, the intensity of strontium aluminates peak gradually stronger which means the crystallization of $SrAl_2O_4$:Eu^{2+} become better. In this paper, there are five kinds of metal matrixes (Cu, Fe, Ni, Mn and Cu-14Al-X) coupled with fluorescent particles ($SrAl_2O_4$:Eu^{2+}, Dy^{3+}) and get five different matrix composite coatings respectively. XRD analysis indicated that the composite coatings with different matrixes are all composed by metal phase and $SrAl_2O_4$. The fluorescent particles do not react with the metal and no impurity phases were observed in sintered coatings as shown in Fig. 2.

3.2 Luminous properties

Figure 3 shows the temperature dependent PL spectra of Cu-14Al-X/$SrAl_2O_4$:Eu^{2+}, Dy^{3+} coatings which were excited with a xenon lamp at a wavelength of 365 nm. The luminous intensity of the coating increases with sintered temperature increase in temperature range of 650–850 °C.
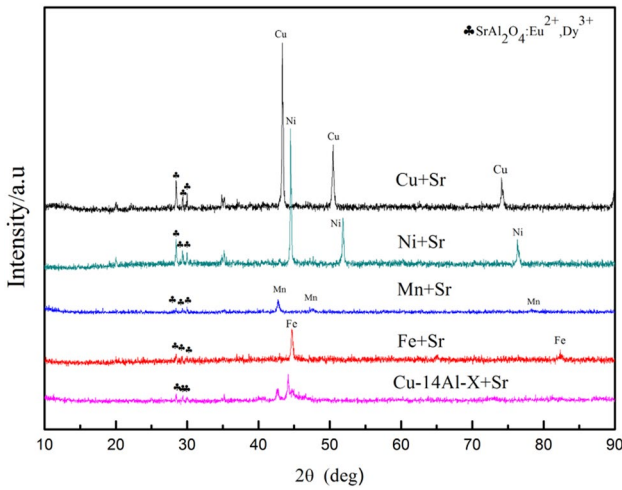
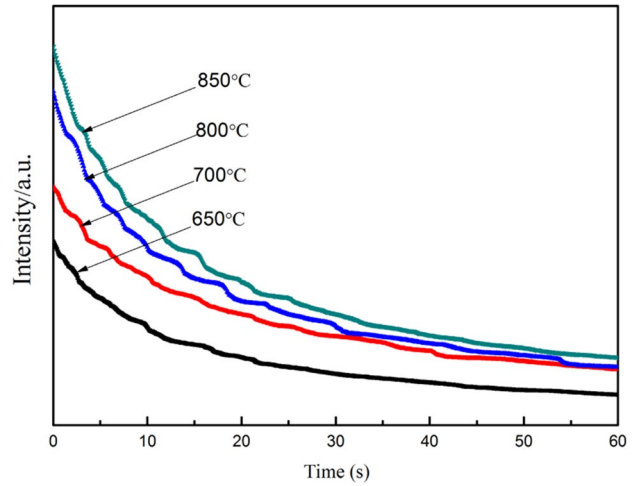**Fig. 2** XRD pattern of the different matrix composite coatings

Fig. 4 Decay *curves* of Cu-14Al-X/SrAl$_2$O$_4$:Eu^{2+}, Dy^{3+} coatings at different sintering temperature
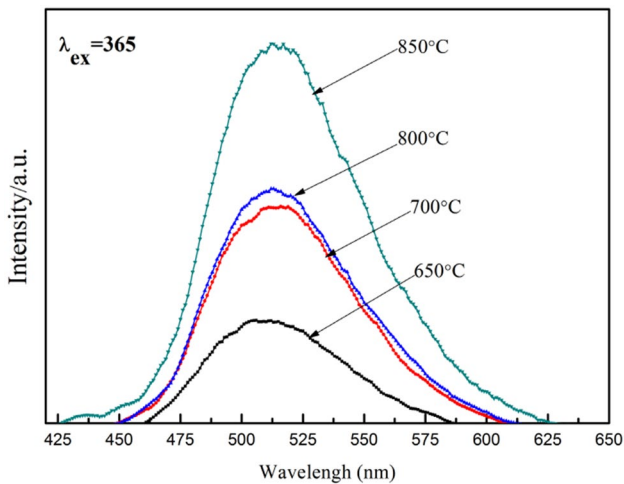
Fig. 3 Emission spectra of Cu-14Al-X/SrAl$_2$O$_4$:Eu^{2+}, Dy^{3+} coatings at different sintering temperature
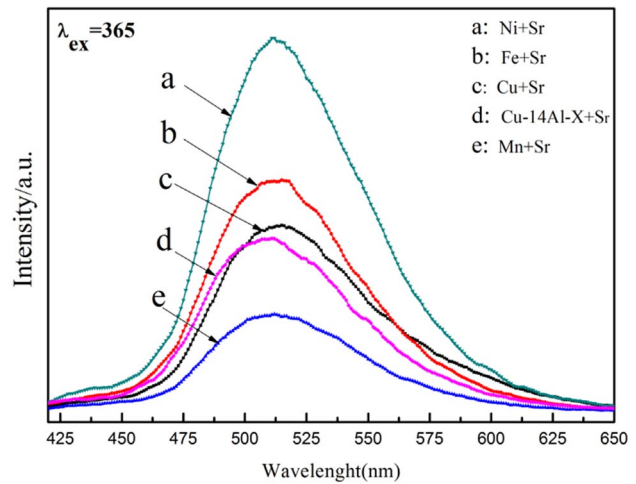

Fig. 5 Emission spectra of different matrix composite coatings

This phenomenon is different from the thermal quenching because the crystallization of SrAl$_2$O$_4$:Eu^{2+}, Dy^{3+} in the coating becomes better, so the luminous enhanced [13]. The emission spectrum of the Cu-14Al-X/SrAl$_2$O$_4$:Eu^{2+}, Dy^{3+} coatings includes a broad band peak at 515 nm corresponding to the green emission. This is the characteristic emission of Eu^{2+} which is attributed to the transition from 4f^{6}5d to the ground state 4f^7. The decay curves of the coatings were shown in Fig. 4, and it is found the initial luminescent intensity is slightly enhanced with increasing of temperature. Those clearly illustrates that the sintered temperature is not major quenching factor for SrAl$_2$O$_4$:Eu^{2+}, Dy^{3+} in the composite coatings.

The emission spectrum of different matrix composite coatings is shown in Fig. 5. Green emission is similar to the coatings at different sintering temperatures. The maximum intensity is Ni/SrAl$_2$O$_4$:Eu^{2+}, Dy^{3+} coating and Mn/SrAl$_2$O$_4$:Eu^{2+}, Dy^{3+} coating has the lowest intensity. Figure 6 shows the decay curve of composite coatings with different metals power. The initial emission intensity of different matrix composite coatings is showed by the order: Ni > Fe > Cu > Cu-14A1-X > Mn. Although the initial brightness of the Fe/SrAl$_2$O$_4$:Eu^{2+}, Dy^{3+} composite coating is high, but fell sharply in the subsequent decay process.

3.3 Quenching mechanism

The trap initial electron density of SrAl$_2$O$_4$:Eu^{2+}, Dy^{3+} in coating is a crucial factor for the quenching, fluorescent particles coupled with different matrix powers show different quenching tendency. If the trap initial electron density is
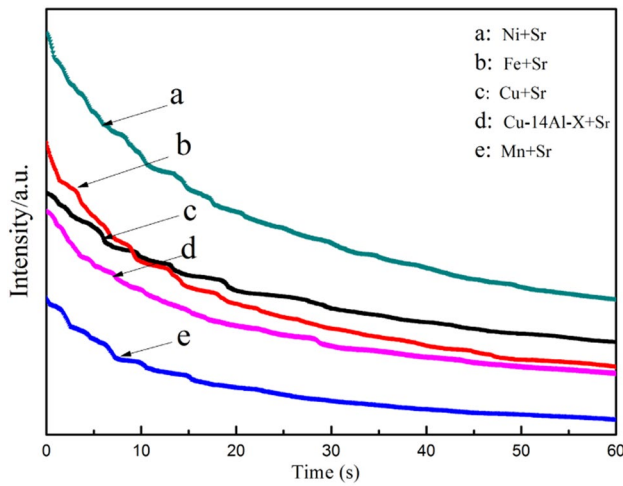
Fig. 6 Decay *curve* of different matrix composite coatings

low, a small number of electrons are needed when excited electrons in the trap come back to the excited state, so initial electron density are stored only in trap energy level and afterglow phenomenon is not easy to be observed in coating [14, 15]. Therefore, the trap initial electron density of $SrAl_2O_4:Eu^{2+}, Dy^{3+}$ is investigated.

The trap initial electron density of $SrAl_2O_4:Eu^{2+}, Dy^{3+}$ is investigated to explore the potential quench mechanism. The persistent luminescence for these metal composite coating has been analyzed by curve fitting. Samples afterglow decay curves satisfy binomial exponential decay equation, which can be described as follow [16]:

$$I = I_0 + I_1 \exp(-t/\tau_1) + I_2 \exp(-t/\tau_2)$$

where I is the phosphorescence intensity, I_0, I_1, I_2 are luminous intensity constants, t is decay time, and τ_1 and τ_2 are the decay times for fast and slow exponential components respectively. The fitting results of composite coatings are tabulated in Table 3.

In the strontium aluminate structure, Dy^{3+} substitute Sr^{2+} formed the point defect (Dy_{Sr}^{**}) which can serve as an effective electron trap having appropriate depth for persistent luminescence. But the electron trap V_O^{**} (inherent oxygen ion vacancies) does not arouse the obvious change of persistent luminescence [17]. In coatings the

intensity of the recombination luminescence and time can be also expressed by the following formula:

$$I(t) = n_0/\tau \exp(-t/\tau) = I_s(-t/\tau)$$

Suppose afterglow decay curves fast decay (I_2, τ_2) from the electronic release in the V_O^{**} trap, and slow decay(I_1, τ_1) was generally related to the electronic release of (Dy_{Sr}^{**}) trap, by the above formula and the available data in the Table 3 can be obtained corresponding the initial concentration of electrons in the trap n_{01}, n_{02}, respectively [18].

As shown in Table 3, the initial electron concentration of pure $SrAl_2O_4:Eu^{2+}, Dy^{3+}$ is higher than that of different matrix composite coatings. It also can be seen that the initial electron concentration in decreasing order of Ni > Cu > Cu-14A1-X > Mn > Fe. This is in line with the emission intensity spectrum of the different matrix composite luminescent coatings except Fe. Some electrons promoted to the 5d levels may get trapped at the V_O^{**} oxygen defects and the trapped electrons lead to occupation of the 5d levels, which results more phosphor valence electron were excited and enhanced luminescence by magnetic energy. The anomalously n_{02} values in Fig. 7 is evident. It is generally accepted that Fe display a wide variety of magnetic behaviors result an oriented rearrangement process of Eu^{2+} during the transition. In the magnetic field, emission peak position is not shifted, but the intensity changes.
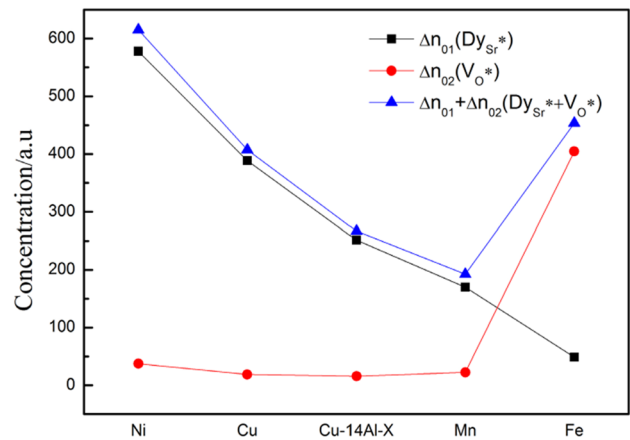

Fig. 7 The concentrations of electrons trapped in (Dy_{Sr}^{**}) and V_O^{**} of different matrix composite coatings

Table 3 Parameters generated in the exponential decay fitting for different metal matrix coatings

Composite coating	τ_1/s	τ_2/s	I_1/a.u.	I_2/a.u.	n_{01}	n_{02}
Mn matrix	29.50137	5.65293	5.75366	3.99327	169.74	22.57368
Ni matrix	35.7263	6.43556	16.17338	5.83842	577.815	37.5735
Fe matrix	7.15868	36.45833	6.81929	11.09872	48.8171	404.64
Cu matrix	38.43773	6.01588	10.1119	3.12421	388.678	18.79
Cu-14Al-X matrix	26.66678	4.50147	9.42704	3.5026	251.38	15.7668

A rudimentary energy level scheme is constructed to explain the contact quenching mechanism of Fig. 8. When the coating after excitation, the luminescent center Eu^{2+} is excited electrons, as well as valence and conduction bands also produce large amounts of electrons and holes which were captured by Eu^{2+}. The contact metal can be as a defect level and dissipation center of electron transition during the energy transfer process, which can capture electrons and reduce the probability of transition of them. Due to the high work function of the contact metal, it can be as a defect level and dissipation center of electron transition during the energy transfer process, which can capture electrons and reduce the probability of transition of them. For different metal composite metals, the work function of different metals is in order: $Ni > Fe > Cu > Cu\text{-}14A1\text{-}X > Mn$. The metal is distributed at different energy levels, so there was also a contact energy barrier between metal particles and $SrAl_2O_4{:}Eu^{2+}$, Dy^{3+}. For $Mn/SrAl_2O_4{:}Eu^{2+}$, Dy^{3+} coating, the electronics in conduction band and excited state of Eu^{2+} from the $SrAl_2O_4{:}Eu^{2+}$, Dy^{3+} fluorescent particles easily transferred to Mn and filled with the energy level of metal. On the contrary, the large contact barrier between Ni and $SrAl_2O_4{:}Eu^{2+}$, Dy^{3+} makes the electrons difficult to cross this barrier and the probability of electrons being captured is small, so the $Ni/SrAl_2O_4{:}Eu^{2+}$, Dy^{3+} composite coating has the highest luminous intensity. This result is consistent with the emission spectrum.

4 Conclusions

In the $Cu\text{-}14Al\text{-}X/SrAl_2O_4{:}Eu^{2+}$, Dy^{3+} coating, the temperature is not a major factor for quenching. The quenching of $SrAl_2O_4{:}Eu^{2+}$, Dy^{3+} phosphors in composite coatings caused by metal contact and the quenching process was modeled. The metal in $Cu\text{-}14Al\text{-}X$ alloy coatings can be as defect level and reduce the effective initial electron trap. Additionally, the different matrix composite coatings present different quenching trends because of work function difference.

Fig. 8 Energy level scheme illustration of metal contact quenching

References

1. Y.M. Huang, Q.L. Ma, Long afterglow of trivalent dysprosium doped strontium aluminate. J. Lumin. **160**, 271 (2015)
2. I.P. Sahu, D.P. Bisen, N. Brahme et al., Luminescence behavior of europium activated strontium aluminate phosphors by solid state reaction method. J. Mater. Sci. **27**, 3443 (2016)
3. B.M. Mothudi, O.M. Ntwaeaborwa, A. Kumar et al., Phosphorescent and thermoluminescent properties of $SrAl_2O_4$:Eu^{2+}, Dy^{3+}, phosphors prepared by solid state reaction method. Phys. B. **407**, 1679 (2012)
4. Y. Zhu, M. Ge, Effect of light conversion agent on the luminous properties of rare earth strontium aluminate luminous fiber. J. Mater. Sci. **27**, 1 (2016)
5. W.S. Li, Z.P. Wang, Y. Lu et al., Mechanical and tribological properties of a novel aluminum bronze material for drawing dies. Wear **261**, 155 (2006)
6. L. Yang, Z. Qiao, W. Li et al., Study of corrosion behavior of powder material of aluminum bronze coatings. P. M. Technol. **28**, 105 (2010)
7. L. He, Q.K. Li, W.S. Li et al., Synthesis and properties of self-sensitization luminescent composite coatings. J. Inorg. Mater. **32**, 56 (2017)
8. C. Muratore, D.R. Clarke, J.G. Jones et al., Smart tribological coatings with wear sensing capability. Wear 265, 913 (2008)
9. M.L. Chithambo, A.H. Wako, A.A. Finch, Thermoluminescence of $SrAl_2O_4$:Eu^{2+}, Dy^{3+}: kinetic analysis of a composite-peak. Radiat. Meas. **97**, 1 (2016)
10. B.M. Mothudi, O.M. Ntwaeaborwa, A. Kumar et al., Phosphorescent and thermoluminescent properties of $SrAl_2O_4$:Eu^{2+}, Dy^{3+}, phosphors prepared by solid state reaction method[J]. Phys. B **407**, 1679 (2012)
11. G. Ju, Y. Hu, L. Chen et al., Concentration quenching of persistent luminescence. Phys. B **415**, 1 (2013)
12. X.F. Yang, G.L. Ning, J. Liu et al., Quenching study on iron impurity in Eu^{2+}, Dy^{3+} doped strontium aluminate phosphor prepared by nano-coating process. J. Rare Earths **25**, 326 (2007)
13. R. Zhang, G. Han, L. Zhang et al., Gel combustion synthesis and luminescence properties of nanoparticles of monoclinic $SrAl_2O_4$:Eu^{2+}, Dy^{3+}. Mater. Chem. Phys. **113**, 255 (2009)
14. B. Cheng, Z. Zhang, Z. Han et al., $SrAl_2O_4{:}Eu^{2+}$, Dy^{3+} nanobelts: synthesis by combustion and properties of long-persistent phosphorescence. J. Mater. Res. **26**, 2311 (2011)

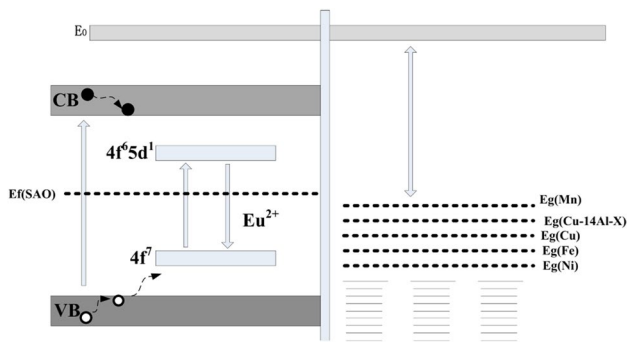15. Z. Zhou, W. Luo, B. Lü et al., Synthesis of high-brightness fine SrAl$_2$O$_4$:Eu, Dy, phosphor by gel-casting and solid-state reaction process. Optoelectron. Adv. Mater. **5**, 125 (2011)

16. S.D. Han, K.C. Singh, T.Y. Cho et al., Preparation and characterization of long persistence strontium aluminate phosphor. J. Lumin. **128**, 301 (2008)

17. X.U. Chao, D.Q. Lu, L.T. Shao et al., Effect of annealling temperature on spectra and trap concentration of SrAl$_2$O$_4$: Eu(2+),Dy(3+) luminescent material. Trans. Mater. Heat Treat. **35**, 19 (2014)

18. T. Jiang, H. Wang, M. Xing et al., Luminescence decay evaluation of long-afterglow phosphors. Phys. B **450**, 94 (2014)